

## Phenylenediamine as Inhibitor in Sour Water at Oil Refinery

Mohammed Hliyil Hafiz<sup>1</sup>, Rana Afif Majed<sup>1</sup>, Rana Sahib Noor<sup>2</sup>, Muthana A. Wehib<sup>2</sup>

<sup>1</sup> University of Technology – Materials Engineering Department. Iraq – Baghdad

<sup>2</sup> Al-Faris State Company – Ministry of Industry and Minerals. Iraq – Baghdad

\*E-mail: [dr.rana\\_afif@yahoo.com](mailto:dr.rana_afif@yahoo.com)

Received: 14 August 2013 / Accepted: 11 October 2013 / Published: 20 October 2013

---

The efficiency of Phenylenediamine (PDA), as corrosion inhibitors for carbon steel (A515) ASTM in sour medium (which obtained from a vacuum distillation unit in Iraqi Oil Refinery that contained dissolved H<sub>2</sub>S and NH<sub>4</sub><sup>+</sup>) at operating temperature (75°C), has been determined by electrochemical measurements. (Open circuit potential OCP, galvanostatic polarization and cyclic polarization) Polarization curves indicate that this amine is anodic inhibitor, which shift corrosion potential toward a noble direction. Four concentrations of phenylenediamine were used to inhibit carbon steel include 1x10<sup>-5</sup>, 1x10<sup>-4</sup>, 1x10<sup>-3</sup> and 1x10<sup>-2</sup> mol/l, protection efficiency calculations indicate that 1x10<sup>-3</sup> M of phenylenediamine gave efficiency equal to 90.45%. The adsorption of phenylenediamine obeys Langmuir adsorption isotherm. Thermodynamics of adsorption (enthalpy of adsorption, the entropy of adsorption and Gibbs free energy) were calculated and discussed. Thermodynamic functions of adsorption processes were calculated from experimental polarization data. The electrochemical results have also been supplemented by optical microscopy, scanning electron microscopy (SEM), and Fourier transforms infrared spectroscopy (FTIR). All the methods employed are in reasonable agreement.

---

**Keywords:** Carbon steel; Corrosion; Sour medium; Inhibition; Amines.

### 1. INTRODUCTION

Sour Water is the wastewater that is produced from atmospheric and vacuum crude columns at refineries. Hydrogen sulfide and ammonia are typical components in sour water that need to be removed before the water can be reused elsewhere in the plant. Removal of these components is done by sending the sour water from the process to a stripping tower where heat, in the form of steam, is applied. The ammonia and hydrogen sulfide contained in the water is released by the heat and exits the top of the tower. The ideal pH value for stripping H<sub>2</sub>S is below 5, since above 5, sulfide is primarily found in the form of ions (HS<sup>-</sup> or S<sup>-2</sup>). Alternatively, efficient ammonia stripping requires a pH above

10 to prevent the formation of ammonium ( $\text{NH}_4^+$ ) ion that cannot be stripped. Although the most favorable strategy for sour water stripping is a three step process where two separate stripper towers are used, one for removing hydrogen sulfide and the other for removing ammonia, economics usually dictate a compromise. Having only one stripper tower and using a pH around 8 allows adequate removal of both gases.

Almost inhibition is used to reduce the corrosion in refinery and there are many studies concerned with corrosion inhibition of steel by different compounds using electrochemical techniques. Ashassi et al. In 2000 investigated two studies about inhibition effects on carbon steel in petroleum/water corrosive mixtures containing of acetic acid and NaCl at 25°C [1,2]. Dharma et al studied the corrosivity of produced water depends on the nature of the dissolved substances. The mitigation of corrosion of carbon steel in the presence of  $\text{CO}_2$ ,  $\text{H}_2\text{S}$  and elemental sulfur were investigated in this study [3]. Abelev et al. studied the effect of  $\text{H}_2\text{S}$  at ppm level concentrations on iron corrosion in 3 wt% NaCl solutions saturated with  $\text{CO}_2$  in the temperature range of 25–85 °C [4]. Sathiyabama et al. studied the inhibition efficiency of Eosin EN in controlling corrosion of carbon steel immersed in well water by mass loss method both in the absence and presence of zinc ion. FTIR spectra indicate that the protective film consists of  $\text{Fe}^{2+}$ —EN complex and  $\text{Zn}(\text{OH})_2$  [5]. Muhammad Shahid and Muhammad Faisal studied the presence of hydrogen sulfide ( $\text{H}_2\text{S}$ ) gas in gas treating plants which increases the severity of corrosion due to the increased aggressiveness [6]. Agus et al. studied corrosion process of carbon steel in chloride solution containing  $\text{H}_2\text{S}$  in the oilfield industry, because it represents the internal corrosion of crude oil pipeline installation [7]. Esparza et al. studied the corrosion behavior of carbon steel AISI 1018 immersed in a sour water sample solution collected from a refinery plant at a temperature between 25 to 50°C with and without stirring [8]. López et al. studied the electrochemical behavior of organic compounds as corrosion inhibitors is being done over a carbon steel AISI 1018 immersed in a corrosive synthetic environment (brine type NACE 1D196), in the absence and presence of hydrocarbon [9]. Laamari et al. studied the efficiency of hexa ethylene diamine tetra methyl-phosphonic acid as a corrosion inhibitor for carbon steel in 0.5 M HCl [10]. Abdel-Rehim et al. studied the corrosion and corrosion inhibition of iron in HCl solutions in the absence and presence of pyrazole (PA) [11]. Ben Hmamou et al. used the gravimetric method to study the temperature effects on carbon steel corrosion in 2M of  $\text{H}_3\text{PO}_4$  in the absence and presence of alizarin red (AZR) [12]. Rivera et al. studied the green corrosion inhibition by a coconut oil-modified imidazoline, namely aminoethyl-amine imidazoline, to investigate the  $\text{H}_2\text{S}$  corrosion inhibition behavior of 1018 carbon steel and compared with a commercial hydroxyethyl-imidazoline [13]. Anthony and Susai studied the environmental friendly inhibitor system arginine- $\text{Zn}^{2+}$  by weight-loss method and FTIR spectral study [14]. Sahaya et al. studied the environmental friendly inhibitor system using a DL - phenylalanine- $\text{Zn}^{2+}$  using FTIR spectra to confirm inhibition [15]. Rivera et al. studied the corrosion inhibition of 1018 carbon steel in 3% NaCl solution at 50°C with imidazoline-based inhibitors [16].

The aim of this work is to inhibit corrosion of carbon steel A515 that is used in manufacturing separation vessels of vacuum distillation unit in the Iraqi oil refinery which in contact with sour water (contained dissolved  $\text{H}_2\text{S}$  and  $\text{NH}_4^+$ ) by phenylenediamine using galvanostatic test to estimate

corrosion parameters. FTIR spectra, SEM and optical microscopy were used to confirm the inhibiting action of phenylenediamine in addition to calculate thermodynamic function of adsorption at 75°C.

## 2. EXPERIMENTAL PART

### 2.1 Materials and solutions

Carbon Steel A515 ASTM was used in this work (chemical composition wt%: 0.165 C, 0.443 Mn, 0.087 Si, 0.007 P, 0.019 S, 0.004 Cr, 0.002 Mo, 0.011 Cu, 0.027 Ni, 0.0008 V, 0.039 W, 0.011 Al and Fe remain) obtained by Spectro MAX. Steel samples with a surface area (1cm<sup>2</sup>) were used in all experiments. The specimen was polished to mirror finish, degreased with acetone and rinsed with distilled water and then mounted by hot mounting using formaldehyde (Bakelite) at 138°C for 8 minutes to insulate all but one side and made a hole on one side of electrical connection. This sample was then dried in open air and stored in desiccators over silica gel for subsequent use.

The base electrolyte was sour water obtained from Al-Dura oil refinery in Iraq from vacuum distillation unit (Separation vessel). Analysis of sour water is listed in Table (1) obtained by many techniques.

**Table 1.** Analysis of sour medium.

Analysis	Amount
Total sulfur by D5453 (S%)	1.261%
Dissolved oxygen	5.81 ppm at 29°C
PH	5.9
Electrical conductivity	116.1 μS/cm
H <sub>2</sub> S content	311 ppm
CO <sub>2</sub> content	< 40 ppm
Naphtha content	2.6 %
H <sub>2</sub> O content	97.41 %
NH <sub>4</sub> <sup>+</sup> content	9.8 ppm
Cl <sup>-</sup> content	102.95 ppm
SO <sub>4</sub> <sup>=</sup> content	70 ppm
TDS	109 ppm

Phenylenediamine was used as corrosion inhibitor with four different concentrations in the sour water medium (1x10<sup>-5</sup>, 1x10<sup>-4</sup>, 1x10<sup>-3</sup>, and 1x10<sup>-2</sup> M). The properties of (PDA) are shown in Table (2).

**Table 2.** Properties of Phenylenediamine.

Property	Phenylenediamine
Molecular formula	C <sub>6</sub> H <sub>8</sub> N <sub>2</sub>
Molar mass g/mol	108.14
Appearance	White crystalline solid, darkens upon exposure to air
Odor	-
Melting point	145-147°C
Boiling point	267°C
Solubility in water	10% at 40°C, 87% at 107°C
Toxicity	Non toxic

## 2.2 Methods

### 2.2.1 Electrochemical measurements

Electrochemical cell was composed of platinum counter electrode, prepared low steel A515 specimen as working electrode and saturated calomel electrode (SCE) as a reference electrode according to ASTM standard cell G5-94 was used [17].

The electrochemical behavior of steel in inhibiting and uninhibited solution was studied by WINKING M Lab potentiostat by recording anodic and cathodic galvanodynamic polarization curves. Measurements were carried out by changing the electrode current automatically from -15 to +15 mA at scan rate 0.1 mA.sec<sup>-1</sup>, while open circuit potential recorded after immersion in test electrolyte for 900 sec. The linear Tafel segments of anodic and cathodic curves were extrapolated to the corrosion potential to obtain corrosion parameters.

### 2.2.2 FTIR measurements

The film formed on the metal surface (after immersing in the sour water medium for 10 days till drying) was carefully removed and mixed thoroughly with KBr. The FTIR spectra were recorded in FTIR-8400S Shimadzu Fourier Transform Infrared Spectrophotometer.

### 2.2.3 Optical Microscopy Examination Study

The carbon steel specimens were corroded in various test solutions containing four different concentrations of inhibitor, the specimens were taken out and dried. The nature of the film formed on the surface of the metal specimen was analyzed by NIKON, ECLIPSE-ME600 Optical Microscope All micrographs are taken at a magnification of 1000x.

### 2.2.4 Scanning Electron Microscopy (SEM)

The VEGAIII TESCAN Scanning Electron Microscope is utilized to document the surface morphology of various specimens of carbon steel (A515) before and after corrosion. All micrographs are taken at a magnification of 500x and 5 kx.

## 3. RESULTS AND DISCUSSION

### 3.1 Open Circuit Potential – Time Measurements

OCP test was recorded after immersion in electrolyte for 900sec. versus SCE. Fig. (1) shows the variety of open circuit potentials ( $E_{oc}$ ) with time for all experimental specimens of carbon steel in sour water medium in the absence and presence of inhibitor with four different concentrations of (75°C). The potential of the sample was followed as a function of time in order to study the evolution of the film chemistry as it came to equilibrium with the solution. Fig. (1) shows the variation of potentials with time were relatively stable and intersected with the behavior in the absence of inhibitor, but can be obtained more positive potentials especially with  $1 \times 10^{-4}$  M (PDA) that get more positive potential than the open circuit potential of the carbon steel in the absence inhibitor.

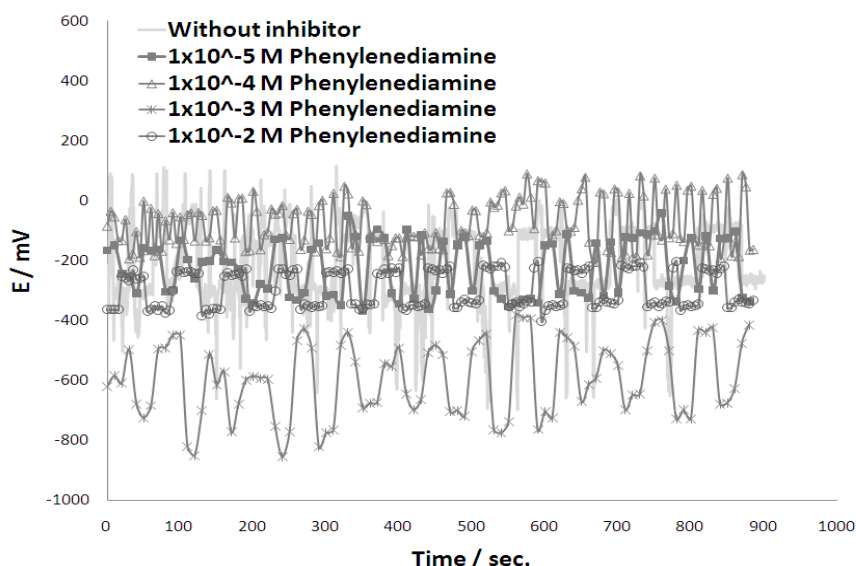


**Figure 1.** Change of potential with time for carbon steel in sour water medium in the absence and presence of four concentrations of (PDA) at 75°C.

### 3.2 Galvanostatic Polarization Measurements

Fig. (2) shows galvanodynamic curves for steel in the absence and presence of four different concentrations of phenylenediamine in sour water at 75°C. These curves indicate the cathodic and anodic regions. At anodic sites, dissolution or oxidation of metals can occur. While at cathodic sites,

many reactions can occur. The main cathodic reduction in acidic medium is the evolution of hydrogen. H<sub>2</sub>S dissolves in water forming a weak acid. The most important cathodic reaction in a sulphide-containing environment produces hydrogen atoms and HS<sup>-</sup>.

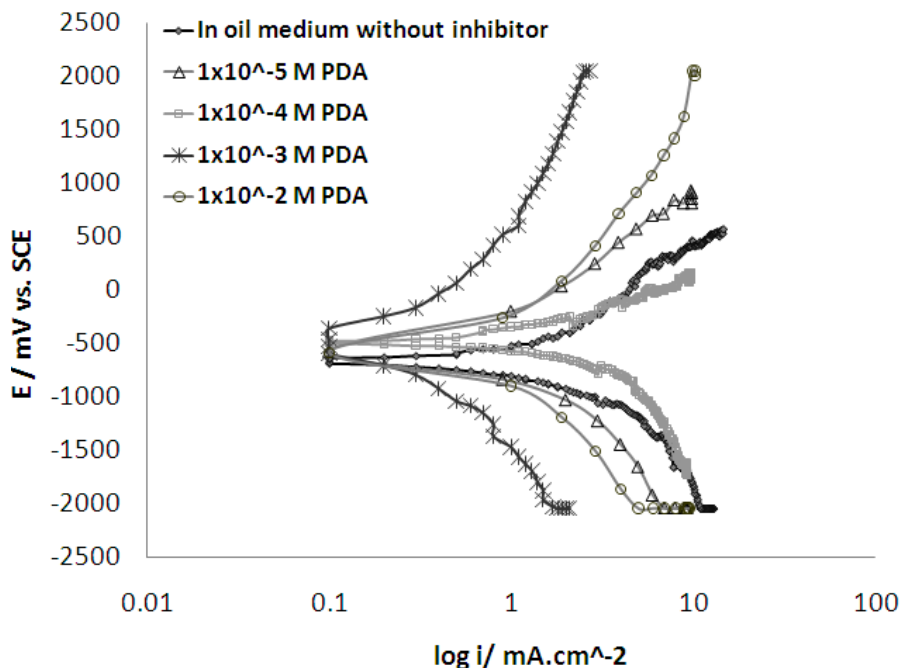


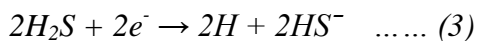
**Figure 2.** Galvanodynamic polarizations of Carbon steel in oil sour medium containing (PDA) with four different concentrations at 75°C.

At anodic sites, oxidation of metals can occur according to the equation:  
 $Fe \rightarrow Fe^{2+} + 2e^- \dots\dots (1)$

While at cathodic sites, many reactions can occur. The main cathodic reduction in normal acidic medium is the evolution of hydrogen as follows:



The most important cathodic reaction in a sulphide-containing environment can be expressed by:



Hydrogen atoms are combined with hydrogen gas, but some hydrogen in the atomic state diffuses into the material.

This may cause hydrogen embrittlement, particularly in high-strength steels. Sulphur originating from H<sub>2</sub>S can affect the corrosion properties of passive materials [18]; sometimes it causes localized corrosion [19].

Corrosion parameters which measured using the Tafel extrapolation method are listed in Table (3) for inhibition steel by phenylenediamine with four different concentrations at 75°C. Corrosion parameters indicate that the presence of phenylenediamine shifts corrosion potentials toward a noble

direction; this means that this amine is anodic inhibitor. The corrosion current densities were decreased.

**Table 3.** Corrosion parameters for inhibition of carbon steel in oil medium include corrosion potential ( $E_{corr}$ ), corrosion current density ( $i_{corr}$ ), cathodic and anodic Tafel slopes ( $b_c$  &  $b_a$ ), corrosion rate ( $C_R$ ) and protection efficiency ( $P\%$ ) at 75°C with four concentrations of phenylenediamine.

Conc. of Inhibitor (M)	$E_{corr}$ mV	$i_{corr}$ $\mu A/cm^2$	Tafel slope ( $mV.dec^{-1}$ )		$C_R$ mm/y	P%
			$-b_c$	$+b_a$		
0	-659.80	2040.0	1400.9	2000.3	23.7	-
$1 \times 10^{-5}$	-583.38	990.90	1840.1	1983.3	11.54	51.43
$1 \times 10^{-4}$	-484.90	416.62	233.8	335.2	4.84	79.58
$1 \times 10^{-3}$	-491.70	194.81	1330.1	1455.4	2.26	90.45
$1 \times 10^{-2}$	-515.00	937.85	2021.2	2035.1	10.9	54.03

The Tafel slopes were very much influenced by the presence of phenylenediamine, and anodic Tafel slopes ( $b_a$ ) have values higher than that of cathodic Tafel slopes. It is inferred that the rate of change of current with change of potential was higher during cathodic polarization than that during anodic polarization.

Protection efficiency P% calculated as follows:

Corrosion rates  $C_R$  in mm/y were calculated according to the following formula:

$$C_{R \text{ mm/y}} = 3.27 \times i_{corr} \times \left(\frac{e}{\rho}\right) \dots\dots\dots (5)$$

Where  $i_{corr}$  is corrosion current density in mA.cm<sup>-2</sup>,  $e$  is equivalent weight of alloy in gram, and  $\rho$  is density of alloy in gm.cm<sup>-3</sup>. The values of corrosion rate were decreased after adding phenylenediamine.

$$P\% = \left[1 - \frac{i_{inhibit}}{i_{uninhibit}}\right] \times 100 \dots\dots\dots (6)$$

Where  $i_{inhibit}$  and  $i_{uninhibit}$  are corrosion current density of inhibited and uninhibited electrolyte. The best concentration of phenylenediamine is  $1 \times 10^{-3}M$  which gave protection efficiency equal to 90.45.

The active (—: NH<sub>2</sub>) group contains a pair of unshared electrons which it donates to the metal surface. The inhibitors react by replacing water molecules by organic inhibitor molecules [20].

Phenylenediamine gave good efficiency, in spite of the presence benzene ring which acts as a drawing group led to reduce the electron density on the nitrogen atom in amine groups which compete water molecules to bond with the metal surface.

### 3.3 Cyclic Polarization Measurements

Cyclic polarization data were recorded by M Lab electrochemical laboratory system with electrochemistry software. Galvanodynamic measurements were carried out in order to determine the initiation and propagation of local corrosion, which is associated with the breakdown of passive protective film.

Fig. (3) Shows cyclic polarization curves of carbon steel in sour medium in the absence and presence of four concentrations of phenylenediamine at 75°C. The data of these curves are in good agreement with the results of galvanodynamic polarization which indicate that the best concentration of the inhibitor that gave the best protection efficiency and the lowest corrosion rate is given the best behavior in cyclic polarization. In other word, the best concentration  $10^{-3}$ M (PDA) which gave the lowest hysteresis loop or it`s disappeared in its cyclic behavior.

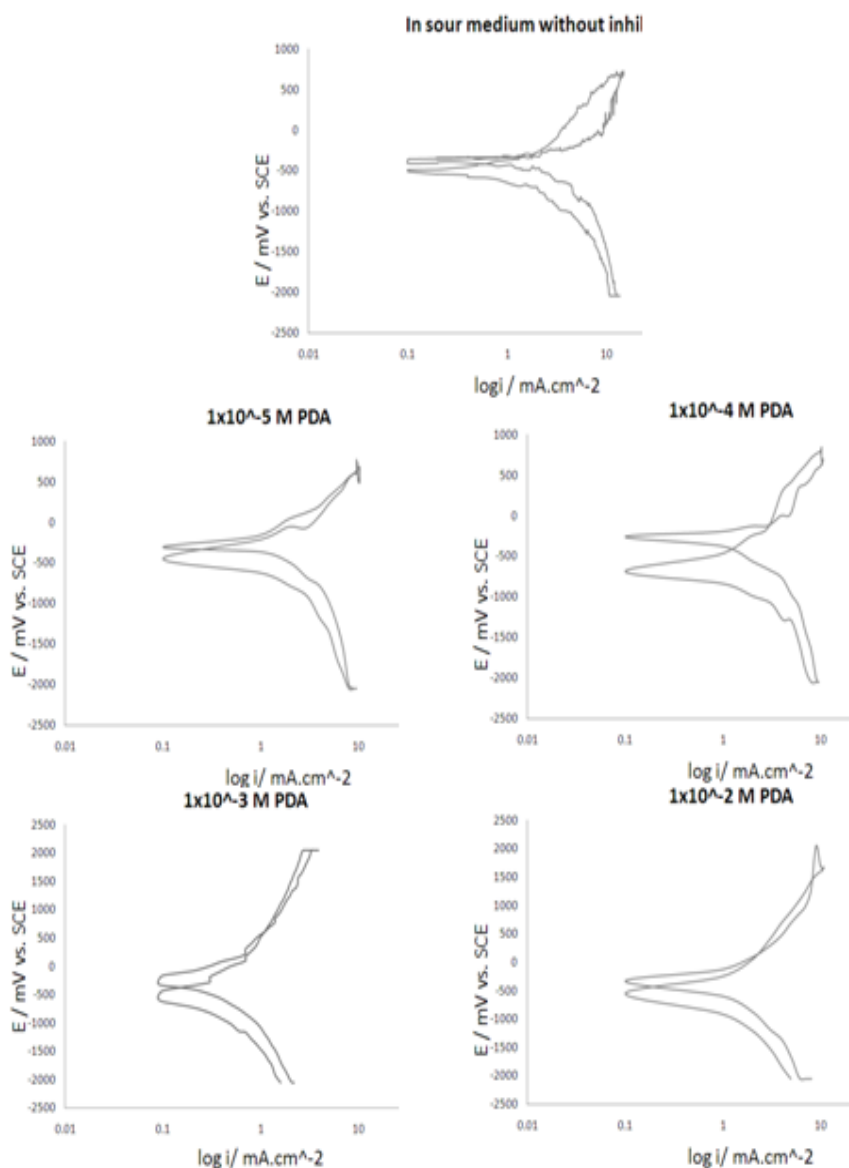


**Figure 3.** Cyclic polarization of Carbon steel in sour water medium containing phenylenediamine with four different concentrations at 75°C.



### 3.4 Adsorption Isotherm

Adsorption depends mainly on the charge and the nature of the metal surface, electronic characteristics of the metal surface, adsorption of solvent and other ionic species, temperature of corrosion reaction and on the electrochemical potential at solution-interface. The most frequently used isotherms include: Langmuir, Frumkin, Temkin, Flory-Huggins, Dhar-Flory- Huggins, Bockris-Swinkels and the recently formulated thermodynamic/kinetic model of El-Awady et al. [21, 22]. The establishment of adsorption isotherms that describe the adsorption of a corrosion inhibitor can provide important clues to the nature of the metal- inhibitor interaction. Adsorption of the organic molecules occurs as the interaction energy between molecule and metal surface is higher than that between the H<sub>2</sub>O molecule and the metal surface [23].

In order to obtain the adsorption isotherm, the degree of surface coverage ( $\theta$ ) for various concentrations of the inhibitor has been calculated according to the equation:

$$\theta = \left[ 1 - \frac{i_{inh.}}{i_{unin.}} \right] \dots\dots (7)$$

The plots of  $C_{inh}/\theta$  against  $C_{inh}$  for the inhibitor at 348 K were straight lines (Fig. 4) indicating that the phenylenediamine obeys Langmuir adsorption isotherm given by the equation:

$$\frac{C_{inh}}{\theta} = \frac{1}{K_{ads}} + C_{inh} \dots\dots (8)$$

Where,  $K_{ads}$  is the equilibrium constant of the adsorption-desorption process,  $\theta$  is the degree of surface coverage and  $C_{inh}$  is the molar concentration of inhibitor in the bulk solution. The apparent free energy of adsorption ( $\Delta G^{\circ}_{ads}$ ) is calculated from the relation:

$$\Delta G^{\circ}_{ads} = -2.303RT \log 55.5 K, \text{ where } K = \frac{\theta}{c(1-\theta)} \dots\dots (9)$$

The values of  $K_{ads}$  and  $\Delta G^{\circ}_{ads}$  are shown in Table (4). The enthalpy of adsorption  $\Delta H^{\circ}_{ads}$  can be calculated from the Gibbs–Helmholtz equation:

$$\left[ \frac{\partial(\Delta G^{\circ}_{ads}/T)}{\partial T} \right]_p = - \frac{\Delta H^{\circ}_{ads}}{T^{\circ}} \dots\dots (10)$$

This equation can be arranged to the following equation:

$$\frac{\Delta G^{\circ}_{ads}}{T} = \frac{\Delta H^{\circ}_{ads}}{T} + K_{ads} \dots\dots (11)$$

**Table 4.** Thermodynamic functions for inhibition of carbon steel in sour water by phenylenediamine at 75°C.

Conc. of Inhibitor (M)	$K_{ads}$	$-\Delta G^{\circ}_{ads}$ kJ.mol <sup>-1</sup>	$-\Delta H^{\circ}_{ads}$ kJ.mol <sup>-1</sup>	$-\Delta S^{\circ}_{ads}$ kJ.mol <sup>-1</sup> K <sup>-1</sup>
1x10 <sup>-5</sup>	105888.4	1203460	38000000	105888
1x10 <sup>-4</sup>	38971.60	442926	14000000	38971.6
1x10 <sup>-3</sup>	9471.204	107644	3403623	9471.2
1x10 <sup>-2</sup>	117.5332	1335.81	42237.4	117.533

The negative values of  $\Delta G^{\circ}_{ads}$  indicated the spontaneous adsorption of phenylenediamine and revealed a strong interaction between inhibitor molecules and metal surface [22,23]. Large values of

$K_{\text{ads}}$  imply more efficient adsorption and hence better inhibition efficiency [24]. The negative sign of  $\Delta H^{\circ}_{\text{ads}}$  in sour water indicates that the adsorption of inhibitor molecule is an exothermic process. Generally, an exothermic adsorption process signifies either physic- or chemisorptions while endothermic process is attributable unequivocally to chemisorptions [22].

The change in entropy can be calculated using the formula of  $\Delta G^{\circ}_{\text{ads}} = \Delta H^{\circ}_{\text{ads}} - T \Delta S^{\circ}_{\text{ads}}$ . The value of  $\Delta S^{\circ}_{\text{ads}}$  is negative indicating that phenylenediamine retained the mobility of metal ions and reducing the dissolution of carbon steel.

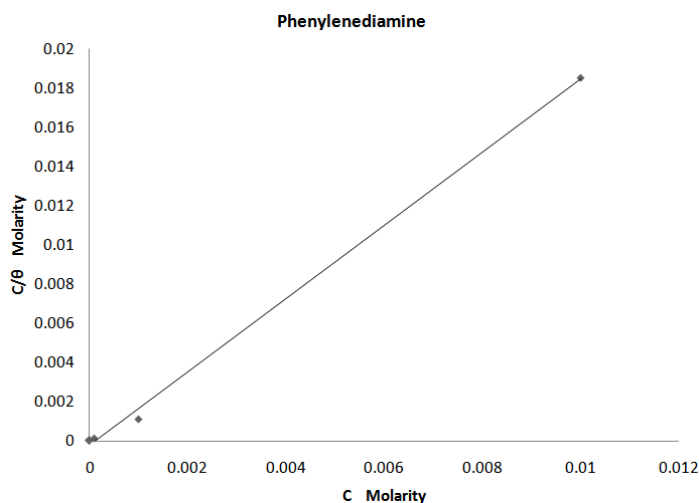
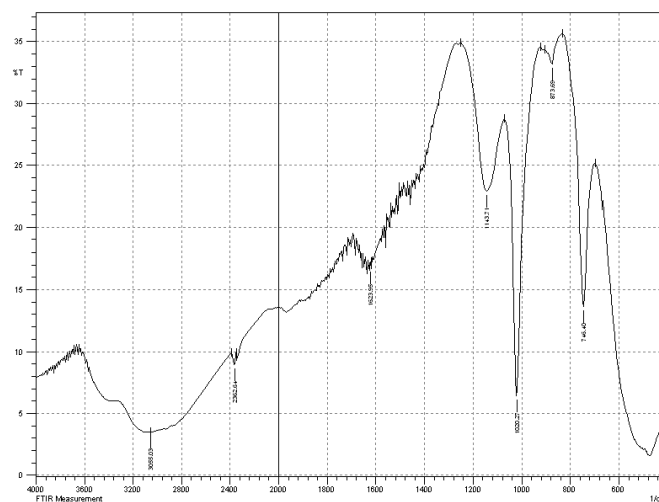


**Figure 4.** Langmuir adsorption isotherm model of phenylenediamine on carbon steel surface at 348 K.

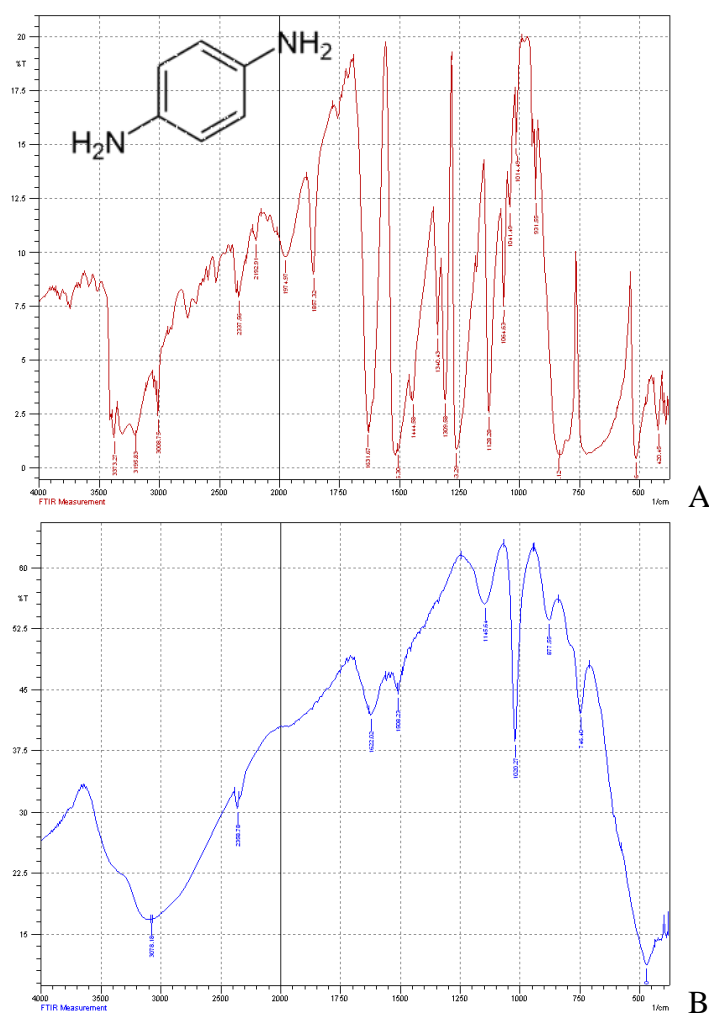
### 3.5 Fourier Transform Infrared Spectra (FTIR)

Fig. (5) shows the FTIR analysis of the film forming on steel surface after corrosion test in oil sour medium at 75°C and this test was measured after immersion in solution for 10 days. The FTIR spectrum indicates appears many peaks, the most important peaks may be due to absorption of compounds contained in the oil medium. The very broad peak at 3055.03  $\text{cm}^{-1}$  may be attributed to O—H stretch (carboxylic acids, alcohols or phenols etc.) and strongly H—bonded which often interferes with C—H absorptions, where if a compound has vinylic, aromatic, acetylenic, or cyclopropyl hydrogen, the CH absorption is to the left of 3000  $\text{cm}^{-1}$ . Weak peak at 2362.64  $\text{cm}^{-1}$  may be due to C≡C stretch because of disubstituted or symmetrically substituted triple bond give no absorption or weak absorption. The most prominent band is that due to C—O stretch at 1020.27  $\text{cm}^{-1}$  in alcohols, ethers or ester. On the other hand, the positive peak at 746.4  $\text{cm}^{-1}$  assigned to  $\gamma\text{-Fe}_2\text{O}_3$ , but disappear the peak at 900 and 1300  $\text{cm}^{-1}$  which assigned to FeOOH that reflect the increase in oxide thickness indicate the continuously corrosion of steel in the oil medium.

Fig. (6-a) shows the FTIR spectrum of phenylenediamine, indicating N—H stretch which occurs in the range from 3500 to 3300  $\text{cm}^{-1}$  with two bands for primary amine. C—H aromatic absorb to the left of 3000  $\text{cm}^{-1}$  and C=C at 1631.67  $\text{cm}^{-1}$ . The N—H bands observed to the right 1500  $\text{cm}^{-1}$  due to NH scissor, C—N stretching and =CH aromatic out-of-plane.



**Figure 5.** FTIR spectrum of Film formed on the carbon steel surface after immersion in the sour medium in the absence of inhibitor for 10 days



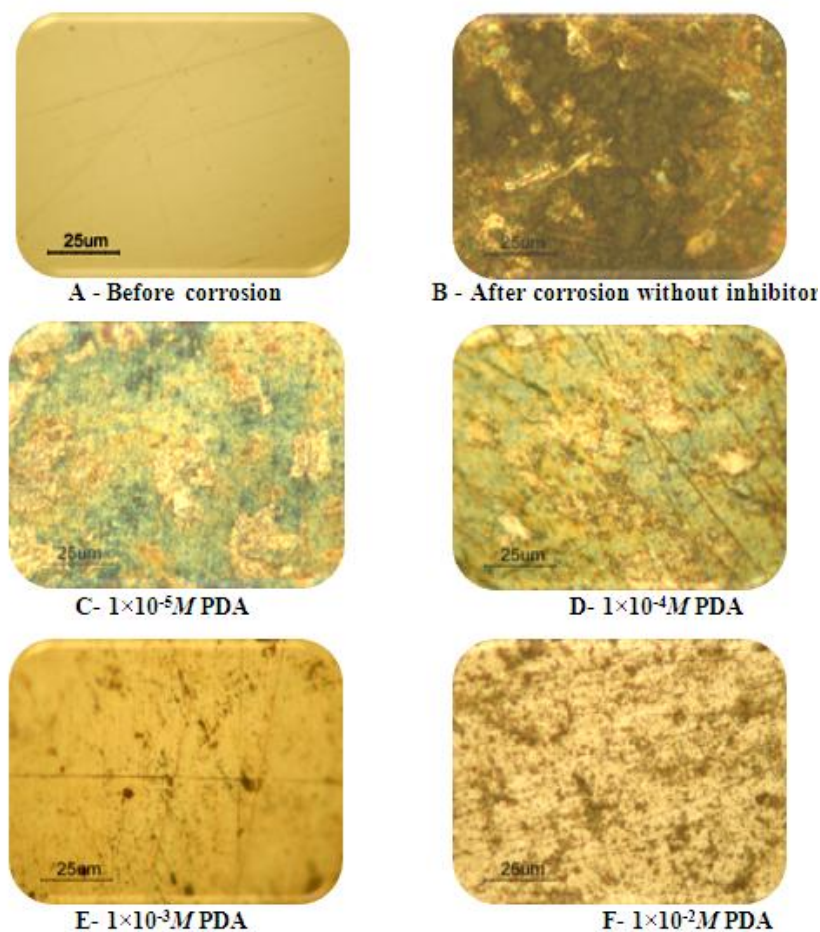
**Figure 6.** FTIR spectrum for phenylenediamine (a), and for film formed on the steel surface after immersion in the sour medium in the presence of  $1 \times 10^{-3}$  M PDA (b).

Fig. (6-b) shows FTIR spectra of the best concentration of phenylenediamine. This spectrum indicates that the stretching frequency of N—H decreased. This suggests that nitrogen of amine group is coordinated with  $\text{Fe}^{2+}$  on the anodic sites of the metal surface, also resulting in the formation of  $\text{Fe}^{2+}$ —N— complex. The C-N stretching frequency shifted to lower values.

Also, can be seen from the FTIR spectrum of the best inhibitor decreasing in broadband that attributed to H-bonded from oil medium, indicating the adsorption of test amine on steel surface competes with water molecules.

### 3.6 Optical Microscopies

The optical microscope test shows the surface of carbon steel before and after adding (PDA) inhibitor with four concentrations of sour water medium at ( $75^{\circ}\text{C}$ ). Fig. (7) shows the optical microscopy of the carbon steel specimen surface which indicates a noticeable reduction in corrosion sites and corrosion products forming on the corroded surface after adding the inhibitor compared with the corrosion in the sour medium without inhibitor especially in the presence of the best concentration  $1 \times 10^{-3}\text{M}$  (PDA) .



**Figure 7.** Optical microscope examination (1000 X) of carbon steel specimen before and after corrosion in the absence and presence of phenylenediamine.

3.7 Electronic Scanning Microscopies (SEM)

Fig. (8) shows SEM image of the surface of the carbon steel specimen after corrosion test at 75°C. The micrograph reveals that, the surface is strongly damaged in the absence of the inhibitors (active corrosion), as shown in Fig. (8-b) While Fig. (8-c) shows an SEM image of the surface of another steel specimen after the same corrosion condition in sour medium containing  $1 \times 10^{-3} \text{M}$  of the phenylenediamine. The micrograph reveals that, there is a decrease in the corrosion sites and pits over the surface, it appears that the surface of the specimen is covered greatly due to the formation of the surface film of the inhibitor. From these observations we can say that the inhibitor give a good inhibition effect for carbon steel and this confirms the results obtained from the other techniques. SEM image performs at two magnitudes 500x and 5 kx.

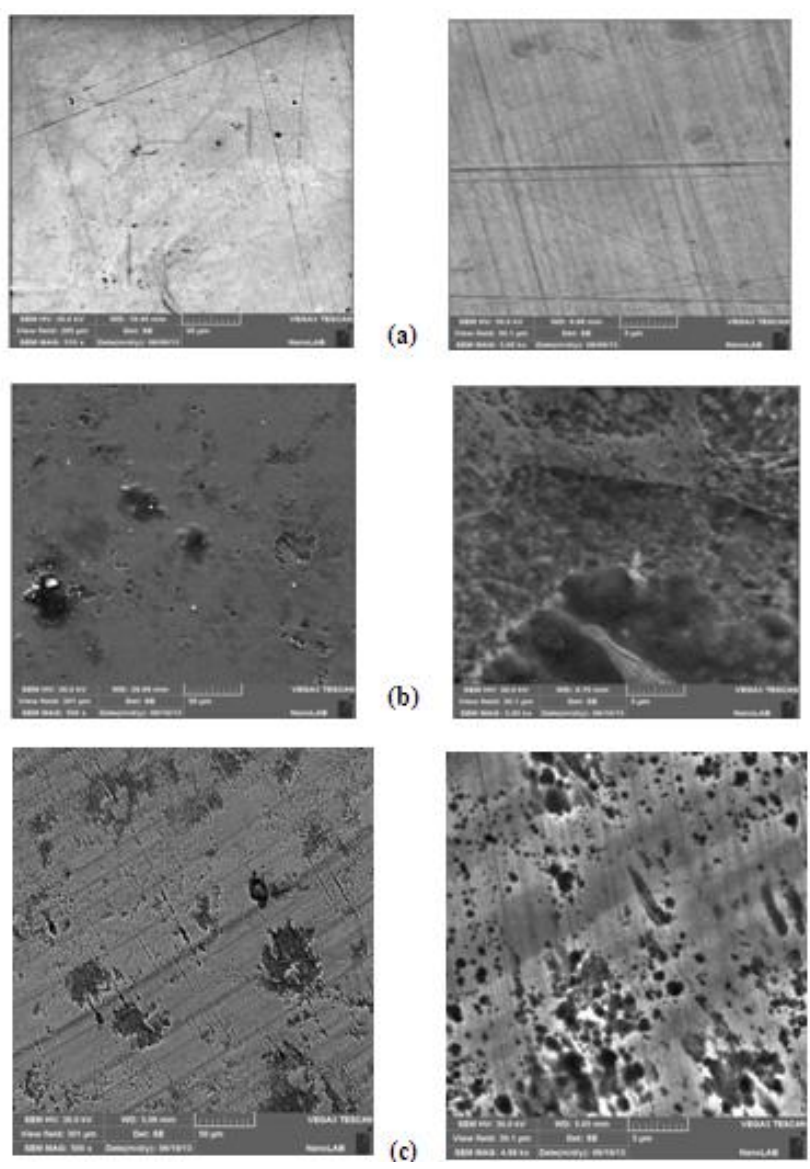


**Figure 8.** Scanning electron micrograph of a steel sample before corrosion (a); after immersion in sour water (b); in sour water containing  $1 \times 10^{-3} \text{M}$  phenylenediamine (c).

#### 4. CONCLUSION

1. All measurements showed that phenylenediamine in sour water behave as a good inhibitor at service temperature 75°C.

2. Galvanodynamic polarization measurements showed that phenylenediamine acts as anodic type inhibitor, where corrosion potential shifts in noble direction.

3. The inhibition efficiencies determined from corrosion current densities and indicate that  $1 \times 10^{-3} \text{M}$  of phenylenediamine gave efficiency equal to 90.45 %, in addition to get acceptable efficiency with other concentrations.

4. The adsorption model obeys the Langmuir isotherm at 348 K. The negative value of  $\Delta G_{\text{ads}}$  indicates that the adsorption of the inhibitor molecules is a spontaneous process and an adsorption mechanism is typical of chemisorptions, while the negative value of  $\Delta H_{\text{ads}}$  indicate exothermic adsorption process which signifies either physic- or chemisorptions.

#### References

1. H. Ashassi-Sorkhabi and S. A. Nabavi-Amri, *Acta Chim. Slov.*, 47(2000) 507.
2. H. Ashassisorkhabi, *Electrochimica Acta*, 47(2002) 2239.
3. A. Dharma, N. Ali, and O. Nihal, *CORROSION*, March (2003) San Diego Ca.
4. E. Abelev J. Sellberg T. A. Ramanarayanan S. L. Bernasek, *J. Mater Sci.*, 44(2009) 6167.
5. J. Sathiyabama, R. Susai, J. Arockia Selvi and J. Jeyasundari, *The Open Corrosion Journal*, 2(2009) 77.
6. S. Muhammad and F. Muhammad, *Arab. J. Sci. and Eng.*, 34(2009).
7. S. Agus, N. Isdiriyani, A. Muljadji, S. Wawang, Proceedings of the Third International Conference on Mathematics and Natural Sciences (ICMNS 2010).
8. E.M. Esparza Zúñiga, M.A. Veloz Rodríguez, J. Uruchurtu Chavarín, V.E. Reyes Cruz, *Int. J. Electrochem. Sci.*, 6(2011) 5016.
9. L. D. López León, M. A. Veloz Rodríguez, V. E. Reyes Cruz, S. A. Pérez García, A.L. López León, *Int. J. Electrochem. Sci.*, 6(2011) 5134.
10. R. Laamari, J. Benzakour, F. Berrekhis, A. Abouelfida, A. Derja, D. Villemin, *Arab. J. Chem.*, 4(2011) 271.
11. S.S. Abdel-Rehim, K.F. Khaled, N.A. Al-Mobarak, *Arab. J. Chem.*, 4(2011) 333.
12. D. Ben Hmamou, R. Salghi, H. Zarrok, A. Zarrouk, B. Hammouti, M. El Hezzat and M. Bouachrine, *Advances in Materials and Corr.*, 2(2012) 36.
13. L.M. Rivera-Grau, M. Casales, I. Regla, D. M. Ortega-Toledo, J.A. Ascencio-Gutierrez, J.G. Gonzalez-Rodriguez, L. Martinez-Gomez, *Int. J. Electrochem. Sci.*, 7(2012) 12391.
14. S.S. Anthony and R. Susai, *J. Electrochem. Sci. Eng.*, 2(2012) 91.
15. A. Sahaya Raja, S. Rajendran, and P. Satyabama, "Inhibition of corrosion of carbon steel in well water by DL-Phenylalanine-Zn<sup>2+</sup> System", *Journal of Chemistry*, 2013, Article ID 720965, 8 pages.
16. L.M. Rivera-Grau, M. Casales, I. Regla, D.M. Ortega-Toledo, J.A. Ascencio-Gutierrez, J. Porcayo-Calderon, L. Martinez-Gomez, *Int. J. Electrochem. Sci.*, 8(2013) 2491.
17. ASTM G5-94 (Reapproved 2004), "Standard Reference Method for Making Potentiostatic and Potentiodynamic Anodic Polarization Measurements".
18. P. Marcus, "Corrosion Mechanisms in Theory and Practice", 2nd Ed., Marcel Dekker, New York, 2002; 287–310.

19. J.A. Enerhaug, "Study of Localized Corrosion in Super Martensitic Stainless Steel Weldments", Thesis, NTNU, Trondheim, 2002.
20. A. Zaki, "Principle of Corrosion Engineering and Corrosion Control", ISBN: 0750659246, Pub. Date: September 2006, Publisher: Elsevier Science & Technology Books, Chapter 6.
21. E. S. Ferreira, C. Giancomelli, F. C. Giacomelli, A. Spinelli, *Mater. Chem. Phys.*, 83(2004) 129.
22. W. H. Li, Q. He, C. L. Pei, B. R. Hou, *J. Appl. Electrochem.*, 38(2008) 289.
23. G. Trabanelli, in: Mansfeld F (Ed.), Corrosion mechanism, Mercel Dekker, New York, 2006.
24. B. Donnelly, T.C. Downie, R. Grzeskowiak, H.R. Hamburg, D. Short, *Corros. Sci.*, 18(1978) 109.